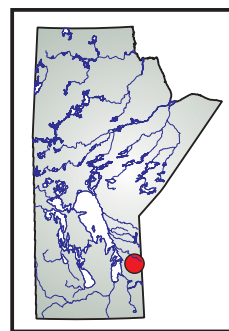


# GS-11 Detailed geological mapping of the Rice Lake mine trend, southeastern Manitoba (part of NTS 52M4): structural geology of hostrocks and auriferous quartz-vein systems

by S.D. Anderson



Anderson, S.D. 2011: Detailed geological mapping of the Rice Lake mine trend, southeastern Manitoba (part of NTS 52M4): structural geology of hostrocks and auriferous quartz-vein systems; in Report of Activities 2011, Manitoba Innovation, Energy and Mines, Manitoba Geological Survey, p. 111–126.

## Summary

The Rice Lake mine trend is located in the central portion of the Archean Rice Lake greenstone belt, and is largely confined to a north-dipping succession of ca. 2.72 Ga volcanoclastic, epiclastic, effusive and synvolcanic intrusive rocks. The trend consists of six significant gold deposits with total reserves and resources of 3.4 million ounces, and total production of nearly 1.6 million ounces. The deposits consist of auriferous quartz-vein systems that are associated with brittle-ductile shear zones and cogenetic arrays of shear and tensile fractures, and preferentially formed within chemically favourable or competent rock types, or along strength-anisotropies, during regional compressional deformation under mid-crustal (greenschist-facies) metamorphic conditions. This report summarizes new results relating to the structural geology of the hostrocks and quartz-vein systems, with emphasis on small-scale examples of shear-associated vein systems exposed on surface.

Structural overprinting and field relationships indicate six distinct generations ( $G_1$ – $G_6$ ) of ductile and brittle-ductile deformation structures in the Rice Lake area, of which only the  $G_3$  and  $G_4$  fabrics are pervasive in the mine trend; these fabrics constrain the structural timing of vein emplacement. Synvolcanic structures include bedding, stratification and a swarm of hypabyssal dikes that locally acted as a significant strength-anisotropy during subsequent deformation. The  $G_3$  deformation structures collectively record intense north-northeast shortening (present co-ordinates) of the mine trend and include a northwest-trending foliation ( $S_3$ ) and northeast-plunging stretching lineation ( $L_3$ ), and a later array of northwest- and northeast-trending brittle-ductile shears (herein called ‘NW shears’ and ‘NE shears’, respectively). Ductile  $G_3$  strain was strongly partitioned into narrow zones of intense non-coaxial shear (sinistral-reverse kinematics) within wider domains of less intense, mostly coaxial shear, which were controlled, at least in part, by primary anisotropy in relatively competent rock types.

Kinematic indicators and associated extension-vein arrays indicate that the NW and NE shears accommodated dextral-normal and sinistral-reverse oblique-slip shear, respectively. Mutual crosscutting relationships indicate that these shears were coeval and at least locally represent a conjugate set, whereas the NW shears in other locations appear to represent subsidiary structures that accommodated rigid-block rotation during

differential slip on through-going NE shears. Transiently higher strain rates or fluid pressures, or strain-hardening effects, during the late increments of  $G_3$  deformation may account for the brittle-ductile nature of these structures. In terms of orientation, style and kinematics, the shears are comparable to northwest- and northeast-trending structures that host major orebodies in the San Antonio/Rice Lake deposit. Hence, the results of this structural study are particularly relevant to deposit modelling and exploration within the Rice Lake mine trend.

## Introduction

The Rice Lake mine trend is located in the central portion of the Archean Rice Lake greenstone belt of the western Superior Province. The mine trend is largely confined to a north-dipping stratigraphic succession of ca. 2.72 Ga felsic epiclastic rocks; mafic volcanoclastic, effusive and synvolcanic intrusive rocks; and intermediate to felsic volcanoclastic rocks. Together these rocks constitute the Townsite unit of the ca. 2.745–2.715 Ga Bidou assemblage. The trend is structurally bounded to the south by the Normandy Creek Shear Zone and to the north by the Wanipigow Shear Zone, and includes six significant deposits with total reserves and resources of 3.4 million ounces (George, 2010). Within these deposits, auriferous quartz veins are associated with brittle-ductile shear zones and cogenetic arrays of shear and tensile fractures that preferentially formed within chemically favourable or competent rock types, or along strength-anisotropies, during regional compressional deformation. With total production of nearly 1.6 million ounces of gold, the Rice Lake mine trend is the most significant lode-gold camp in Manitoba and is currently the focus of intensive exploration and mining activity by San Gold Corporation. The San Antonio/Rice Lake deposit at Bissett is the largest deposit in the trend and accounts for most (~1.5 million ounces) of the past gold production.

As described in the companion report (Anderson, GS-10, this volume), the geology and structure of a roughly 6 km<sup>2</sup> area north and northeast of Rice Lake were mapped in detail (1:5000 scale) during a 4-week campaign in August 2011. This work was undertaken to address the need for a single comprehensive map of the Rice Lake mine trend at a scale suitable for detailed modelling of the

contained gold deposits. Anderson (GS-10, this volume) and the accompanying preliminary map (Anderson, 2011) provide a summary of results pertaining to the lithology and stratigraphy of the hostrocks, whereas this paper summarizes new results relating to the structural geology of the hostrocks and quartz-vein systems, with particular emphasis on small-scale examples of shear-associated vein systems exposed on surface in the north-central portion of the mine trend.

## Regional setting

The Rice Lake greenstone belt is located in the western segment of the Uchi Subprovince in the western Superior Province. In Manitoba, the Uchi Subprovince is flanked to the north by Mesoarchean and Neoproterozoic tonalite, granodiorite and granite of the Wanipigow River plutonic complex, and minor Mesoarchean supracrustal rocks of the North Caribou Terrane (Percival et al., 2006a, b). To the south, the belt is bounded by Neoproterozoic metasedimentary rocks, derived gneiss and granitoid plutonic rocks of the English River Subprovince. The Wanipigow Shear Zone (WSZ) defines the northern boundary of the belt, whereas the southern boundary is defined by the Manigotagan Shear Zone. Both of these structures are interpreted to represent long-lived crustal-scale ‘breaks’ of the type associated with major orogenic gold districts in other Archean greenstone belts. In the Rice Lake area, major subsidiary structures to the WSZ include the Gold Creek, Normandy Creek and Red Rice Lake shear zones.

## Stratigraphic setting of the mine trend

At Rice Lake, the Rice Lake greenstone belt consists of subaqueously deposited intermediate to felsic volcanoclastic and epiclastic rocks, with subordinate basaltic effusive and synvolcanic intrusive rocks, of the ca. 2.745–2.715 Ga Bidou assemblage. These rocks define an upright stratigraphic succession that dips moderately to the north and is divided for descriptive purposes into four lithostratigraphic units. From south to north, these are the Independence Lake, Rainy Lake road, Townsite and Round Lake units (Figure GS-11-1). Geochemical signatures indicate a systematic variation in basalt chemistry from Fe-tholeiitic (mid-ocean-ridge basalt [MORB] like) near the base of the succession to evolved calcalkalic (arc like) near the top, which is interpreted to indicate an extensional eruptive setting within a volcanic arc (Anderson, 2008). These rocks are intruded from the south by synvolcanic tonalite–granodiorite plutons of the ca. 2.725–2.715 Ga Ross River plutonic suite and are unconformably overlain to the west by crossbedded arenite and polymictic conglomerate of the ca. 2.7 Ga San Antonio assemblage, which was deposited in a fluvial-alluvial basin shortly after cessation of major volcanism.

The Townsite unit is the major host to gold mineralization in the Rice Lake area and largely defines the Rice Lake mine trend (Figure GS-11-2). It varies from steeply northwest dipping in the east to moderately northeast dipping in the west, and thus defines a broad arcuate map pattern. This unit is approximately 1.3 km thick at Rice Lake and tapers out toward the east along strike, possibly as a result of structural thinning near the confluence of the WSZ and Normandy Creek Shear Zone (Figure GS-11-1). To the west, this unit is truncated from the north by a deep erosional scour at the base of the Round Lake unit and from the south by the basal unconformity of the San Antonio assemblage. Felsic volcanic sandstone and heterolithic volcanic conglomerate constitute the lower section of the unit and are interstratified toward the north with mafic to intermediate flows and associated volcanoclastic rocks. Using local mine terminology, these rocks correspond to the ‘Hares Island formation’ and ‘Shoreline basalt’, respectively. The epiclastic rocks contain a unimodal population of ca. 2.724 Ga detrital zircons (Anderson, 2008) and are intruded by gabbro sills and slightly discordant dikes, the thickest of which hosts the San Antonio/Rice Lake deposit and is informally referred to as the ‘SAM unit’. The upper section of the unit consists of coarsely plagioclase-phyric, intermediate to felsic volcanoclastic rocks and is referred to as the ‘Townsite dacite’. Each of these map units hosts economic concentrations of gold.

## Structural setting of the mine trend

As described by Anderson (2008), structural overprinting and field relationships indicate six distinct generations ( $G_1$ – $G_6$ ) of ductile and brittle-ductile deformation structures in the Rice Lake area. Only the  $G_3$  and  $G_4$  fabrics are pervasive; they record regional deformation under mid-crustal (greenschist-facies) metamorphic conditions and are well developed throughout the mine trend. The  $G_1$  and  $G_2$  fabrics are locally developed only outside the mine trend. The  $G_5$  and  $G_6$  fabrics are regional and retrograde, and tend to be poorly developed in the mine trend. Nevertheless, each generation is described briefly below (after Anderson, 2008) to provide context for the structural description of the mine trend. Planar fabrics, linear fabrics and folds are herein denoted by  $S_x$ ,  $L_x$  and  $F_x$ , respectively, where ‘x’ indicates the assigned generation.

### $G_1$ structures

The earliest fabric generation in the Rice Lake area is observed in fragments of phyllite in a clastic dike near the base of the Townsite unit. Very fine grained phyllosilicate minerals in these fragments define a penetrative foliation ( $S_1$ ) that pre-dates entrainment in the dike and appears to record dynamic recrystallization in the lower greenschist facies. A possible source of these fragments is located

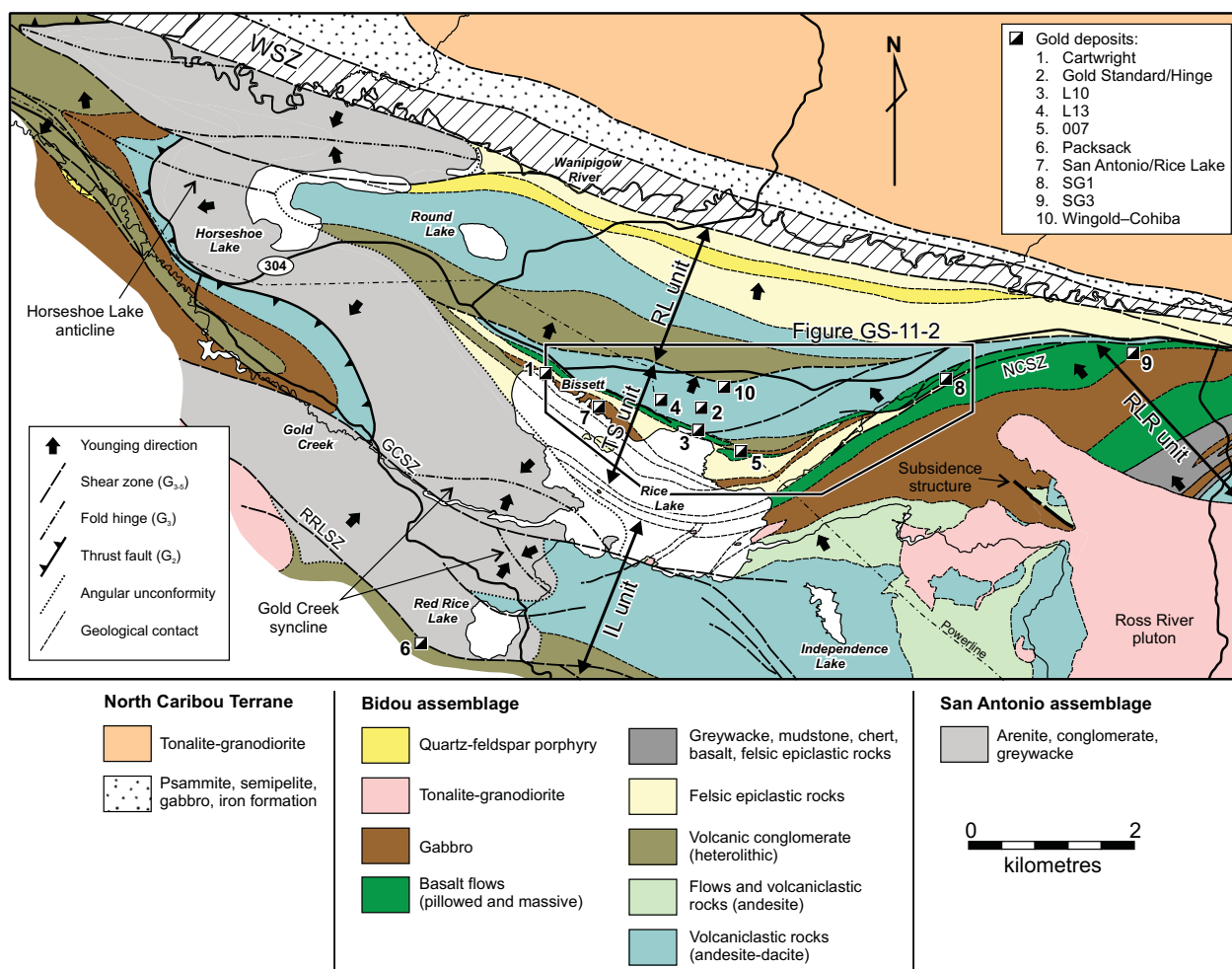


**Figure GS-11-1:** Simplified geology of the Rice Lake area, showing the locations of the Independence Lake (IL), Rainy Lake road (RLR), Townsite (TS) and Round Lake (RL) units of the Bidou assemblage, and the major gold deposits. Abbreviations: GCSZ, Gold Creek Shear Zone; NCSZ, Normandy Creek Shear Zone; RRLSZ, Red Rice Lake Shear Zone; WSZ, Wanipigow Shear Zone (indicated by hachured pattern).

along strike to the east, where map patterns and facies associations indicate a highly discordant fault at the contact between the Independence Lake and Round Lake units (Figure GS-11-1). This fault appears to have channelled hypabyssal intrusions and volcanogenic massive sulphide (VMS)-style hydrothermal alteration, and is thus interpreted to represent a synvolcanic subsidence structure related to extension and rifting of the volcanic arc; it is assigned to the first ( $G_1$ ) generation of structures.

Early tilting and exhumation of the volcanic arc is indicated by a pronounced angular discordance between primary stratification in the Bidou assemblage and the basal unconformity of the San Antonio assemblage (Figure GS-11-1). This tilting was possibly related to regional-scale accretionary processes; however, no mesoscopic deformation structures are recognized from this early event.

### $G_2$ structures

Structures of the second generation ( $G_2$ ) consist of a weak layer-parallel foliation ( $S_2$ ) that is developed in the San Antonio assemblage, particularly along its upper contact. At this contact, west-younging clastic rocks of the San Antonio assemblage are structurally overlain to the west by west-younging volcanic rocks of the Bidou assemblage (Figure GS-11-1). This older-over-younger map pattern is interpreted to indicate the presence of a  $G_2$  thrust fault, which possibly formed in response to accretionary processes or in the initial stages of crustal thickening related to collisional orogenesis.

### $G_3$ structures

Structures of the third generation ( $G_3$ ) are pervasive in the Rice Lake area and formed at mid-crustal depths in response to regional compression. The Bidou assemblage contains a pervasive planar-linear (S-L) shape fabric

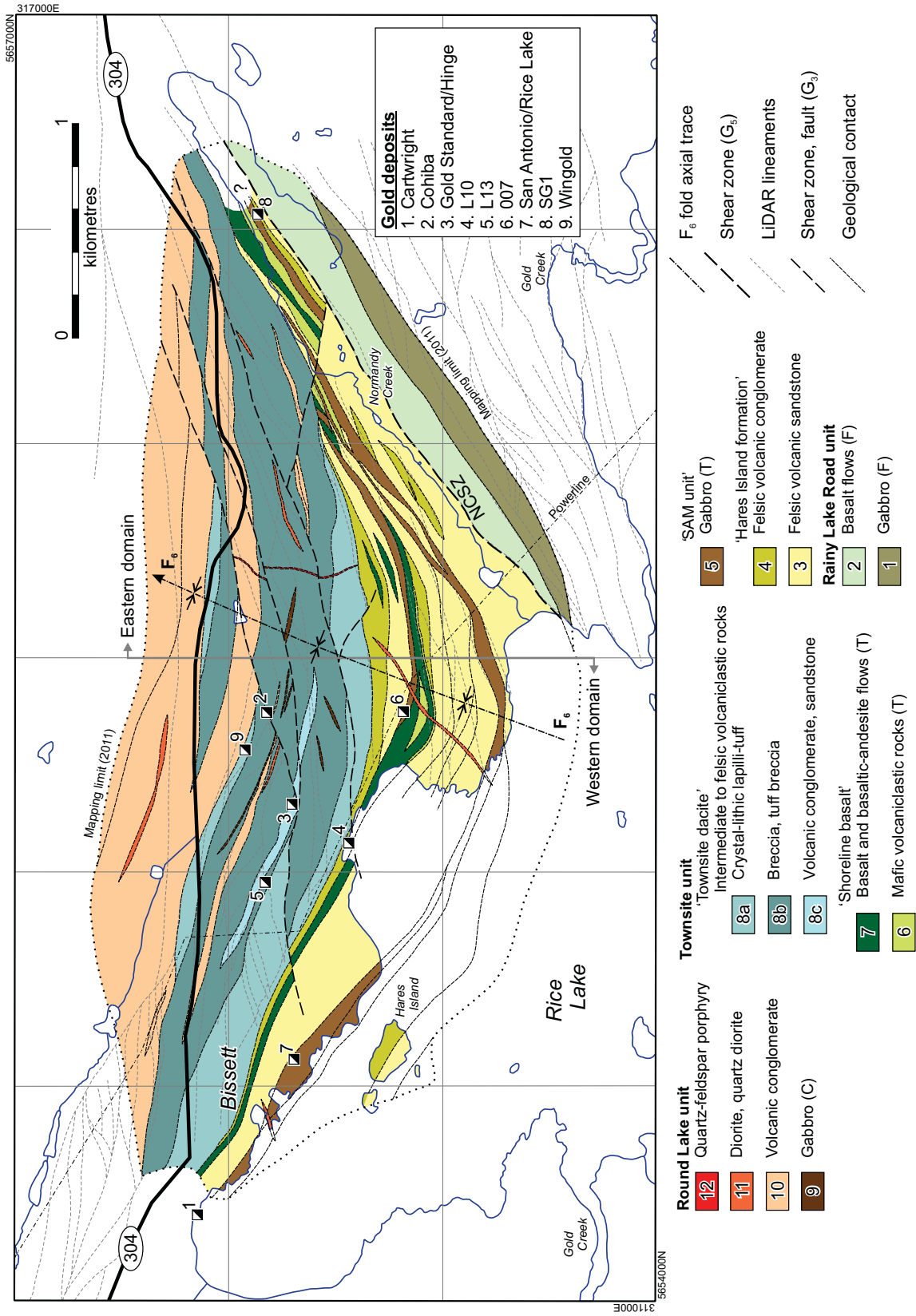


**Figure GS-11-2:** Geology of the Rice Lake mine trend, simplified from PMAP2011-3 (Anderson, 2011). Major gold deposits are shown in the approximate locations of their up-dip projections to surface. Abbreviations: C, calcalkalic; F, Fe-tholeiitic; LiDAR, light detection and ranging; NCSZ, Normandy Creek Shear Zone; T, transitional tholeiitic-calcalkalic.

defined by flattened and stretched primary features. The shape fabric typically includes a continuous foliation defined by fine-grained chlorite, actinolite and sericite. The  $S_3$  fabric generally trends west-northwest and dips steeply to moderately north. The associated  $L_3$  stretching lineation plunges moderately to the northeast in the plane of the  $S_3$  fabric. At Rice Lake, the  $S_3$  fabric is consistently oriented at a very shallow counter-clockwise angle to bedding (which thus faces east on  $S_3$ ) and mesoscopic examples of  $F_3$  folds are very rare; the  $G_3$  shape fabric is generally symmetric and is thus interpreted to indicate the predominance of pure shear over simple shear. From north to south across the Rice Lake area, the  $L_3$  lineation exhibits a systematic change in trend and plunge, from steeply or moderately northeast plunging in the south to shallowly east plunging in the north, which is interpreted to result from reorientation during transcurrent shear along the WSZ (Poulsen et al., 1986).

West of Rice Lake, the  $S_3$  fabric passes continuously into the San Antonio assemblage, where it is most prominently defined by flattened pebbles; the  $L_3$  fabric is generally not well developed in these rocks. The  $S_3$  fabric is axial planar to the Horseshoe Lake anticline (HLA) and Gold Creek syncline (GCS), which are the most prominent closures in a macroscopic train of  $F_3$  folds that trends across the structural grain of the belt (Figure GS-11-1). These folds are tight, steeply inclined structures that are overturned to the southwest. The GCS plunges shallowly to the northwest, whereas the HLA plunges steeply to the north. On the shared limb of the HLA and GCS south of Horseshoe Lake, the  $S_3$  fabric is refracted toward the west-southwest. The macroscopic  $F_3$  fold train terminates at the angular unconformity and does not extend into the underlying Bidou assemblage. This relationship indicates that the maximum principal stress during folding was oriented subparallel to the unconformity but suborthogonal to strata in the underlying volcanic units. Hence, the clastic rocks accommodated the regional shortening by buckling and folding, with some flattening, whereas the volcanic rocks experienced flattening and subvertical stretching without buckling. On a regional scale, the geometry and kinematics of the  $G_3$  structures indicate northeast-southwest shortening (present co-ordinates) of the Rice Lake belt, which was likely coeval with major crustal thickening and collisional orogeny in the western Superior Province. As described below, the geometry, kinematics and structural timing of brittle-ductile shears and associated auriferous quartz veins in the mine trend indicate that they were emplaced during the late stages of the deformation that produced the  $G_3$  shape fabric.

#### ***G<sub>4</sub> structures***

Throughout the Rice Lake area, the  $S_3$  fabric is overprinted by a finely spaced crenulation cleavage that is assigned to the  $G_4$  generation. The  $S_4$  cleavage trends

west or southwest, dips steeply northwest and typically strikes 20–30° counter-clockwise to the  $S_3$  fabric. The  $S_4$  cleavage transects meso- and macroscopic  $F_3$  folds in the San Antonio assemblage, and intersects  $S_3$  to form a prominent crenulation lineation that generally plunges at moderate angles to the northeast. The  $S_4$  fabric is axial planar to rare, open to tight, Z-asymmetric folds that plunge moderately north. The  $G_4$  structures overprint alteration and auriferous vein systems in the mine trend and appear to have accommodated weak northwest-southeast shortening of the Rice Lake belt, perhaps during the early increments of the regional, late-orogenic, dextral transcurrent-shear deformation that characterizes the major belt-bounding shear zones (see below).

#### ***G<sub>5</sub> structures***

Fifth-generation ( $G_5$ ) ductile-deformation structures are pervasive in the Rice Lake area but are only penetrative in discrete high-strain zones, the most notable of which are the regional-scale Wanipigow Shear Zone and its subsidiary splays (the Gold Creek, Normandy Creek and Red Rice Lake shear zones; Figure GS-11-1). The  $G_5$  high-strain zones are characterized by penetrative mylonitic foliations ( $S_5$ ) defined by foliated sericite, chlorite and domains of dynamically recrystallized quartz and feldspar. These zones are subvertical and trend west-northwest to north-northwest, except where overprinted by later structures (see below). Quartz-filled pressure fringes, stretched clasts, quartz ribbons or ridge-in-groove striations define a prominent linear fabric that plunges to the northwest. Packets of strongly Z-asymmetric, open to tight, upright, chevron-style  $F_5$  folds are a characteristic feature of the  $G_5$  high-strain zones and plunge variably, from shallowly east to steeply north. On the margins of the  $G_5$  high-strain zones, the  $S_5$  fabric is locally manifested as a spaced shear-band cleavage that trends northwest or north-northwest and dips subvertically. Dextral kinematic indicators are well developed on horizontal outcrop surfaces and typically include S-C fabrics,  $\sigma$ -porphyroclast systems, shear bands and asymmetric boudins. The geometry of the  $G_5$  structures indicates that they accommodated regional north-northwest-south-southeast shortening that was strongly partitioned into discrete zones of dextral transcurrent-shear deformation.

#### ***G<sub>6</sub> structures***

The latest generation of ductile deformation ( $G_6$ ) is associated with an open upright syncline that trends north through the Rice Lake area (Figure GS-11-2). In the hinge of this fold, a weak crenulation cleavage ( $S_6$ ) is locally associated with upright symmetric folds that plunge at moderate angles to the northeast. The  $S_6$  cleavage generally dips steeply to the east-southeast and is best developed along the south shoreline of Rice Lake. The  $G_6$  structures accommodated east-west shortening, perhaps

in response to a buttressing effect along the northwestern margin of the Ross River pluton during the late increments of north-northwest–south-southeast shortening of the belt. Collectively, the  $G_4$ ,  $G_5$  and  $G_6$  structures are interpreted to record broadly progressive deformation within a regional regime of late-orogenic dextral transpression.

### Detailed structural geology of the mine trend

Deformation structures throughout the Rice Lake mine trend were examined in detail during the 2011 mapping program in order to gain an improved understanding of the structural evolution, particularly as it relates to the orientation, style, kinematics and structural timing of quartz-vein systems. Improved access and exposure in key areas of the mine trend, which are the result of intensive exploration activity since the most recent Manitoba Geological Survey (MGS) mapping program (Anderson, 2004, 2005), facilitated mapping on a more detailed scale. The efficiency of this mapping was further improved by the use of high-resolution airborne light detection and ranging (LiDAR) data and orthorectified aerial photographs, both of which were recently acquired by San Gold Corporation and generously provided to MGS for this project. Digital-elevation models of the ‘bare-Earth’ surface derived from the LiDAR data were used to construct shaded-relief images that proved particularly useful for identifying outcrop, planning traverses and delineating bedrock structure in areas of poor exposure. A preliminary structural interpretation of these images was exported to a hand-held GIS and ground-checked in the field using GPS. In outcrop, the topographic linears identified in the LiDAR data were generally found to coincide with slightly discordant dikes and/or discrete ductile or brittle-ductile shear zones.

The following structural descriptions are accompanied by lower-hemisphere, equal-area projections of structural data collected from outcrop during the 2011 field season, augmented by data collected during the 2004–2005 mapping program. On the basis of prevailing orientations, these data are divided into two structural domains (west and east), the boundary between which coincides with line 314000E of the Zone 15 UTM grid (Figure GS-11-2). These data are further subdivided into generations, which are correlated on the basis of orientation, style and overprinting relationships with the regional generations of structure.

As noted above,  $G_1$  and  $G_2$  structures are only observed outside the mine trend. The  $G_3$  and  $G_4$  structures are pervasive throughout and constrain the structural timing of gold mineralization, as described in detail below. The  $G_5$  structures are pervasive within the Normandy Creek Shear Zone, which coincides with a prominent topographic low that extends northeast from the east end of Rice Lake. These structures are only well exposed in underground workings in the SG1 mine, where they

clearly overprint gold mineralization and record intense ductile strain associated with reverse-dextral (northwest-side-up) non-coaxial shear within zones of chloritic or sericitic mylonite and ultramylonite (Anderson, 2008). From west to east along the mine trend,  $G_3$ – $G_5$  structures exhibit systematic changes in orientation and thus define the open  $F_6$  syncline that trends in a northerly direction through the east end of Rice Lake. The  $G_5$  and  $G_6$  structures are not described further here.

### Synvolcanic structures

Bedding and stratification in the western domain of the Rice Lake mine trend generally strike to the west-northwest and dip moderately to the northeast (Figure GS-11-3a), whereas primary structures in the eastern domain generally strike to the west-southwest and dip steeply to the northwest (Figure GS-11-3g). Single examples of overturned bedding in both the western and eastern domains appear to result from local drag or block-rotation effects adjacent to discordant structures (see below). In both domains, primary structures are crosscut by mafic to intermediate dikes that are commonly oriented at a shallow ( $\sim 10$ – $20^\circ$ ) counter-clockwise angle to bedding (Figure GS-11-3b, h); a distinctive quartz-feldspar porphyry dike in the eastern domain is oriented at a slightly higher angle to bedding. Strike directions of the dikes vary more widely ( $\sim 90^\circ$ ) than those of bedding in both domains, and their dips are generally steeper. Given the textural evidence for hypabyssal emplacement (Anderson, GS-10, this volume), the oblique orientations of the dikes with respect to bedding may indicate an unusual upper-crustal stress regime during emplacement (i.e., the minimum principal stress was neither horizontal nor vertical), or that they were transposed into these orientations during subsequent deformation.

### Ductile $G_3$ structures

The earliest recognized deformation structure in the mine trend is the pervasive  $S_3$ - $L_3$  shape fabric, which is defined by flattened and stretched clasts and pillows, and a continuous foliation of fine-grained chlorite, actinolite and sericite (Figure GS-11-4a). The  $S_3$  fabric in the western domain generally strikes to the west-northwest and dips steeply or moderately to the northeast, whereas this fabric in the eastern domain generally strikes to the west-southwest and dips steeply to the northwest (Figure GS-11-3c, i). In both domains, the  $S_3$  fabric crosscuts primary structures at a very shallow ( $\sim 5^\circ$ ) counter-clockwise angle (the upright beds thus face east on  $S_3$ ) and dips slightly more steeply than bedding. No examples of mesoscopic  $F_3$  folds of bedding were observed in the mine trend. The associated  $L_3$  stretching lineation is very well developed throughout and is most prominently defined by plagioclase crystals in the Townsite dacite (Figure GS-11-4b); in some locations, these rocks are

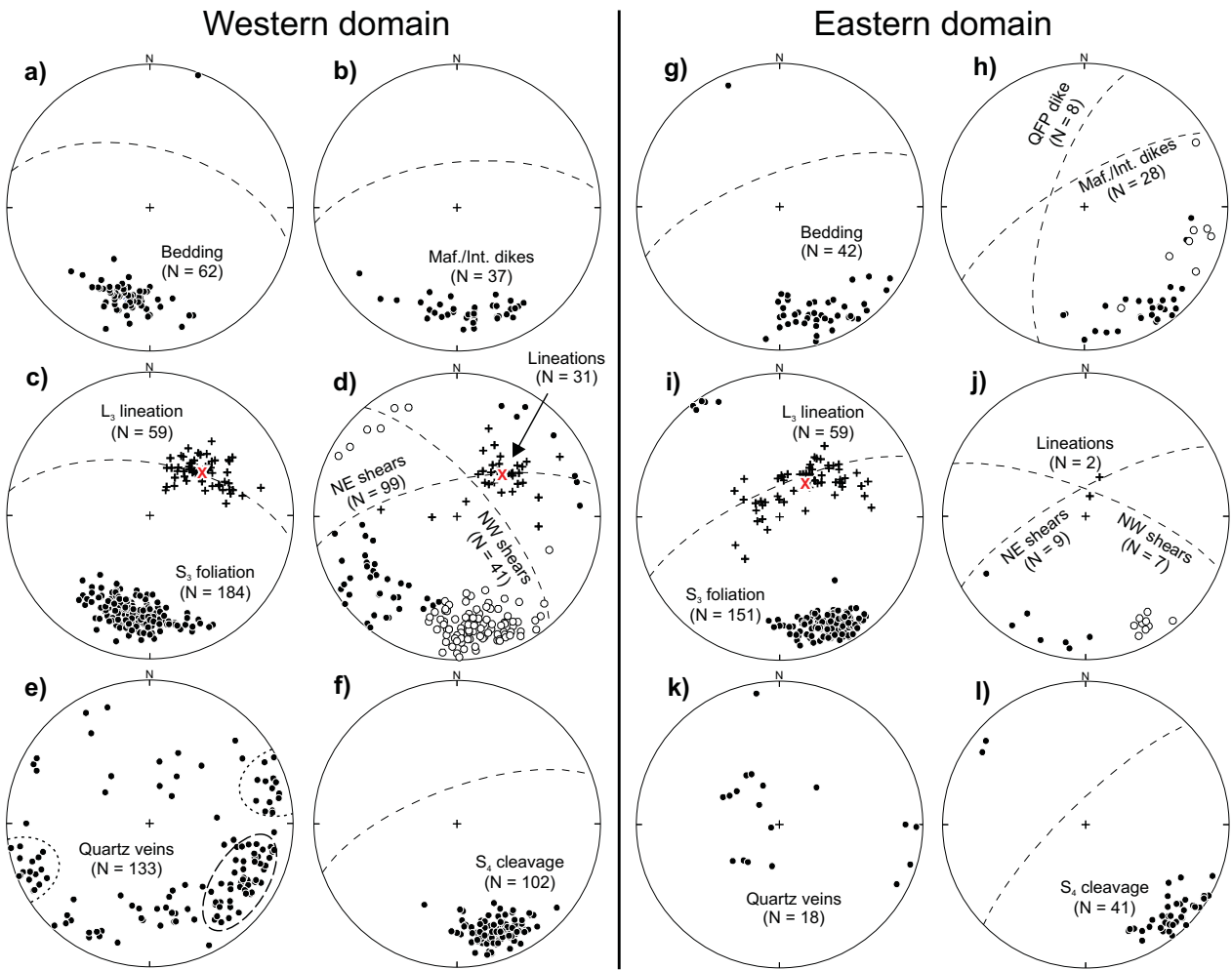


**Figure GS-11-3:** Lower-hemisphere, equal-area projections of structural data in the western (a–f) and eastern (g–l) domains of the mine trend: **a**) and **g**) poles to bedding; **b**) and **h**) poles to contacts of mafic and intermediate dikes; quartz-feldspar porphyry dikes in eastern domain indicated by open circles; **c**) and **i**)  $L_3$  linear fabric (crosses; mean orientation indicated by red 'X') and poles to  $S_3$  planar fabric (circles); **d**) and **j**) poles to northwest-trending shears (NW shears; filled circles) and northeast-trending shears (NE shears; open circles), with associated slickenline or chlorite lineations (crosses; mean orientation indicated by red 'X'); **e**) and **k**) poles to quartz veins; ellipses indicate the two main clusters in the data from the western domain; long-dashed ellipse indicates extension veins associated with NE shears, whereas short-dashed ellipse indicates extension veins associated with NW shears; **f**) and **l**) poles to the  $S_4$  crenulation cleavage. Great circles (dashed lines) indicate the mean orientation of the corresponding planar structures. Abbreviations: Int., intermediate; Maf., mafic.

$L>S$  tectonites. The  $G_3$  shape fabric locally intensifies into narrow (<2 m) widely spaced zones of chloritic or sericitic mylonite that contain intense S-L fabrics and appear to record distinctly higher  $G_3$  strain than the surrounding rocks.

Local asymmetric fabrics and folds in these zones indicate sinistral-reverse non-coaxial shear (Figure GS-11-4c); these zones are interpreted to represent ductile precursors to the brittle-ductile shears described below. Outside these zones, the  $G_3$  shape fabric is less intense and generally symmetric (e.g., Lau and Brisbin, 1996); hence,  $G_3$  strain appears to have been strongly partitioned on a macroscopic scale (Anderson, 2008). The  $L_3$  lineation

has a very consistent orientation in the western domain and plunges moderately to the northeast in the plane of the  $S_3$  fabric (Figure GS-11-3c). The orientation of the  $L_3$  fabric in the eastern domain shows significant scatter (Figure GS-11-3i), which is interpreted to result from reorientation during late-stage ( $G_3$ ) reverse-dextral shear along the Normandy Creek Shear Zone.

### **Brittle-ductile $G_3$ structures**

The  $G_3$  shape fabric is overprinted throughout the mine trend by discrete brittle-ductile shear zones and shear fractures (hereafter referred to as 'shears') that are separated into two distinct sets on the basis of

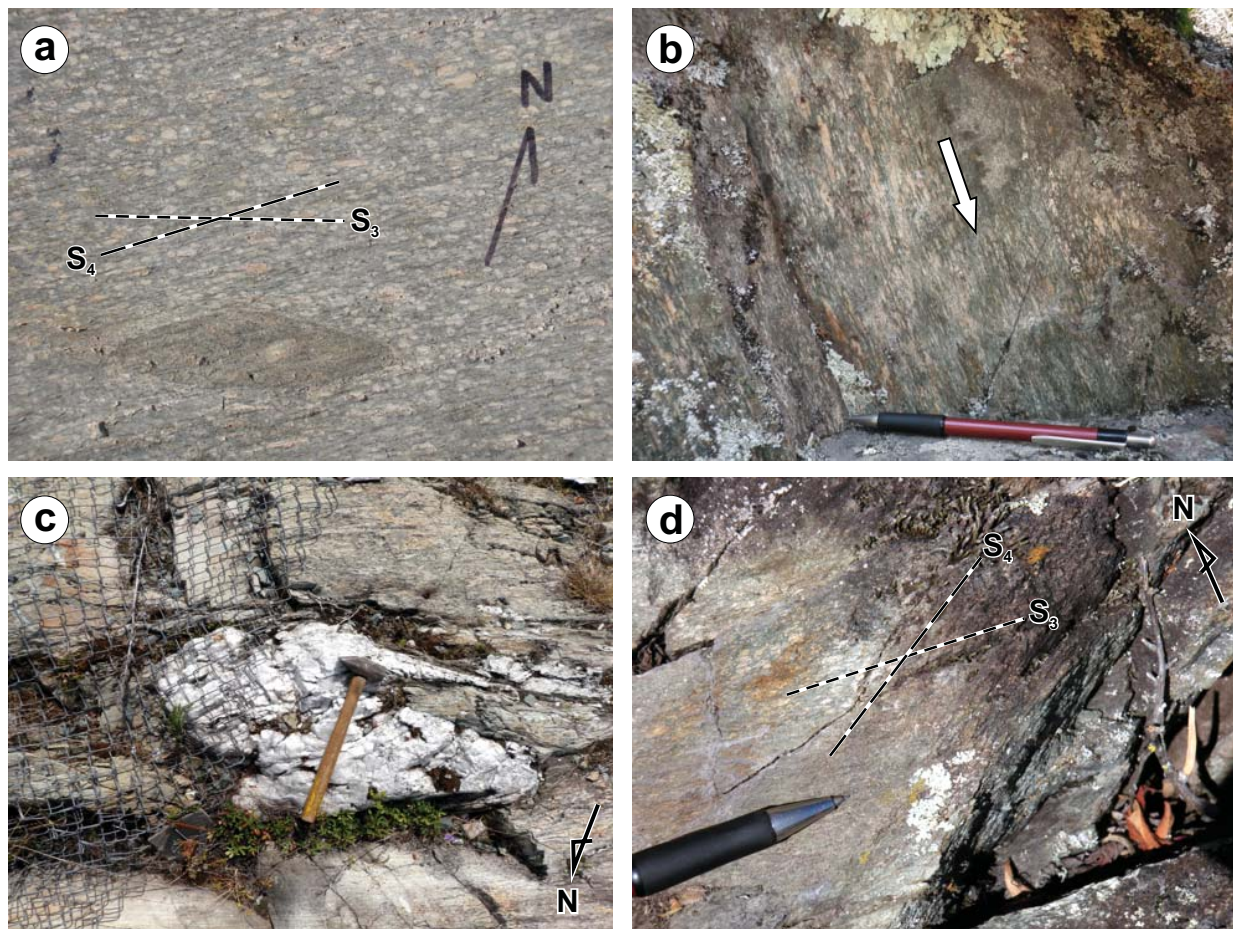


**Figure GS-11-4:** Outcrop photographs of deformation structures in the Townsite dacite: **a)** penetrative  $S_3$  shape fabric (defined by flattened clasts and aligned plagioclase phenocrysts) overprinted by finely spaced  $S_4$  cleavage, eastern domain (clast is ~10 cm in length); **b)** penetrative  $L_3$  fabric defined by stretched plagioclase crystals, western domain; **c)** rootless, isoclinal S-fold in  $G_3$  high-strain zone, eastern domain; the fold asymmetry is compatible with sinistral shear; **d)** overprinting relationships between the shape fabric in a  $G_3$  high-strain zone and the  $S_4$  crenulation cleavage, western domain.

orientation and kinematics. Mutual overprinting and crosscutting relationships between the two sets indicate that they evolved synchronously. The orientation, style and kinematics of these shears are comparable to the northwest- and northeast-trending structures that host the major orebodies in the San Antonio/Rice Lake deposit, which are described by Reid (1931), Stockwell (1938), Gibson and Stockwell (1948), Poulsen et al. (1986), Lau (1988), Lau and Brisbin (1996) and Rhys (2001).

#### Northeast-trending shears (NE shears)

The NE shears are well developed throughout the mine trend. Ground-checks of the preliminary structural interpretation of the LiDAR data indicate that these shears generally coincide with topographic lineaments, particularly where they follow early mafic or intermediate dikes. The most prominent of these shears are shown on Figure GS-11-2. In the western domain, the NE shears

strike to the west-southwest and dip steeply or moderately to the northwest, whereas they strike to the southwest and dip steeply to the northwest in the eastern domain (Figure GS-11-3d, j). Within both domains, the NE shears have fairly consistent orientations: they cut at a shallow counter-clockwise angle across primary structures and the  $S_3$ - $L_3$  shape fabric, and are oriented roughly parallel to mafic and intermediate dikes (Figure GS-11-5a, b). The latter relationship may indicate that the NE shears were controlled, at least in part, by the anisotropy of the dikes.

Highly variable field characteristics of individual NE shears appear to relate to different stages of development in a progressive deformation. Incipient NE shears are marked by en échelon arrays of synthetic shear or extension fractures. At an early stage of development, these fractures were joined by discrete, through-going shear fractures, which are typically marked by planar slip-surfaces and discontinuous seams

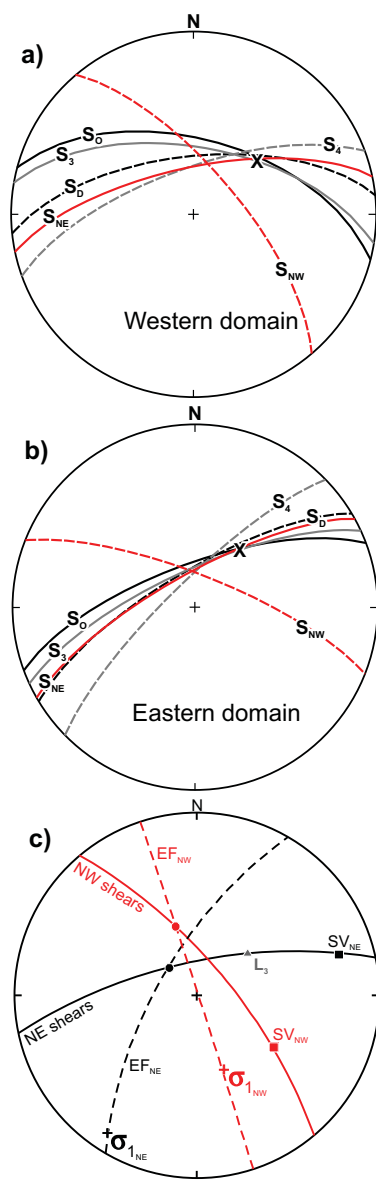


**Figure GS-11-5:** Lower-hemisphere projections showing the mean orientations of structures in the mine trend: **a)** western domain and **b)** eastern domain; equal-area plots; mean orientations of planar structures are indicated by great circles; 'X' indicates the mean orientation of the  $G_3$  linear fabric;  $S_0$ , bedding and stratification (solid black lines);  $S_0'$ , contacts of mafic and intermediate dikes (dashed black lines);  $S_3$ ,  $S_3'$  planar shape fabric (solid grey lines);  $S_4$ ,  $S_4'$  crenulation cleavage (dashed grey lines);  $S_{NE}$ , northeast-trending shears (NE shears; solid red lines);  $S_{NW}$ , northwest-trending shears (NW shears; dashed red lines); **c)** detailed geometry of structures associated with NW and NE shears in the western domain; equal-angle plot; EF, mean extension fracture; SV, slip-vector (calculated to be perpendicular to the line of intersection between the mean shear plane and extension fracture);  $\sigma_1$ , maximum principal stress (calculated); structures in the eastern domain are not included in this analysis, as they deviate significantly from regional trends on the eastern limb of the macroscopic  $F_6$  fold and the associated extension veins (Figure GS-11-3k) are comparatively poorly developed.

of cataclasite. This progression is clearly evident at the lateral tips of NE shears (Figure GS-11-6a), which dissipate along strike into en échelon or horsetail arrays of shear or extension fractures, and abruptly terminate at wing cracks (Figure GS-11-6b). In later stages of development, the shears are characterized by continuous, strongly foliated zones of chloritic or sericitic mylonite that range up to several metres in thickness and contain discontinuous fault-fill quartz veins (Figure GS-11-6c). The fault-fill veins vary from laminated to brecciated to massive, and locally contain stylolitic pressure-solution seams marked by concentrations of fine-grained pyrite, tourmaline and chlorite. Slickenlines and chlorite lineations on slip-surfaces and foliation planes plunge moderately to the northeast, roughly parallel to the  $L_3$  fabric in the wallrocks. Pressure fringes on pyrite cubes in narrow sulphidization haloes surrounding the fault-fill veins also parallel the  $L_3$  lineation. The external  $S_3$  shape fabric is either sharply truncated at the margins of the shears or is continuously transposed into parallelism with the internal fabric.

Most shears are associated with diffuse peripheral arrays of en échelon extension fractures (quartz filled) that vary from planar to prominently sigmoidal (S-asymmetric; Figure GS-11-6d). In the western domain, the lateral tips of these fractures typically strike to the southwest and dip steeply northwest (Figure GS-11-3e). Asymmetric fabrics (Figure GS-11-6c), offset markers and dilational jogs (Figure GS-11-6b, e) indicate sinistral-reverse oblique-slip shear, which is compatible with the geometry of the peripheral extension veins. Apparent displacements are generally less than 10 m, but range up to approximately 50 m for the thickest, most-continuous shears. The bulk-slip vector calculated from the mean orientations of the NE shears and associated extension fractures in the western domain plunges shallowly to the east-northeast (Figure GS-11-5c), at a significant angle to lineations in the shear planes (Figure GS-11-3d). This discrepancy may be due to reactivation or may indicate a non-ideal stress configuration during shearing (e.g., the intermediate principal stress,  $\sigma_2$ , may not have coincided with the shear plane; Blenkinsop, 2008).

#### Northwest-trending shears (NW shears)

The NW shears are also developed throughout the mine trend, but tend to be thinner, less continuous and more widely spaced than the NE shears. Ground-checks of the preliminary structural interpretation of the LiDAR data indicate that the NW shears coincide with topographic lineaments that also tend to be more subtle and less continuous than those associated with the NE shears. The one exception to this occurs in the eastern domain, where a major NW shear is traced along strike for 900 m (Figure GS-11-2). In the western domain, the NW shears typically strike to the northwest and dip steeply or moderately to the northeast (Figure GS-11-3d) but also include a minor

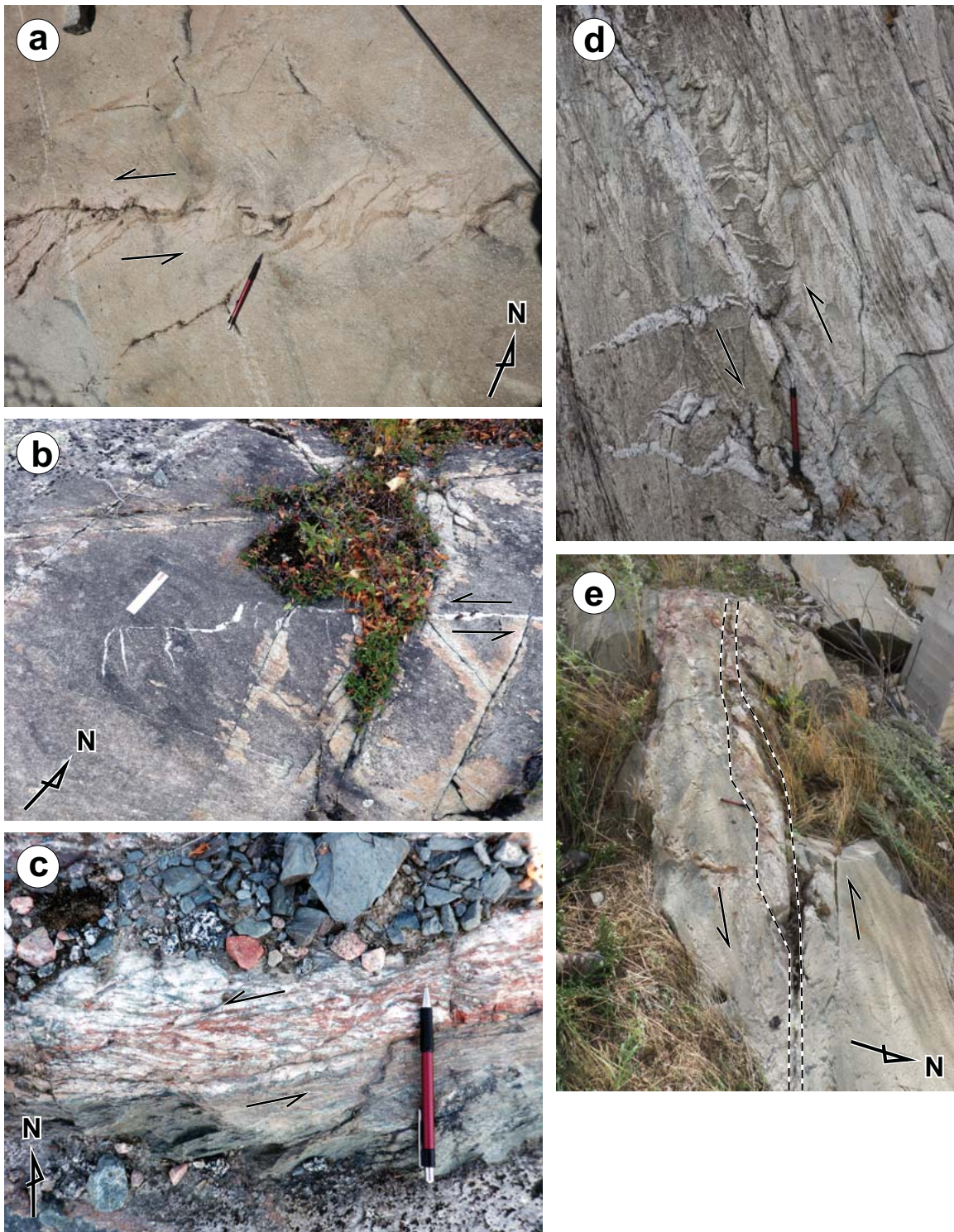


**Figure GS-11-6:** Outcrop photographs of small-scale northeast-trending shears (NE shears): **a)** northeastern lateral tip, showing progression from en échelon sigmoidal extension and synthetic shear fractures (right) to a discrete slip-surface bounded by extension fractures (left), Hinge portal; **b)** southwestern lateral tip, showing wing cracks at the lateral termination of a discrete shear fracture (marked by narrow fault-fill quartz vein), 100 m northwest of the Wingold deposit; note left-stepping dilational jog; 15 cm ruler for scale; **c)** discrete ductile shear, showing penetrative chlorite foliation and well-developed fault-fill quartz veins, 400 m north of the Wingold deposit; asymmetric fabric indicates sinistral shear; **d)** vertical exposure, showing discrete shear fracture (marked by fault-fill quartz vein from upper left to lower right) and peripheral en échelon arrays of planar and sigmoidal extension veins, 250 m west of the Wingold deposit; vein asymmetry indicates north-side-up shear; **e)** discrete shear with fault-fill quartz vein in left-stepping dilational jog, SAM unit at the A-shaft headframe; note pencil for scale at the south contact of the vein.

subset of shears that dip steeply to the southwest. In the eastern domain, they strike to the west-northwest and dip steeply to the northeast (Figure GS-11-3j). Within both domains, the NW shears consistently crosscut primary structures and the  $S_3$ - $L_3$  shape fabric at a clockwise angle (Figure GS-11-5a, b) but tend to be more variable in orientation than the NE shears. The apparent absence of a pre-existing anisotropy in the northwest direction may explain the comparatively poor development and variable orientations of the NW shears.

In most locations, these shears are characterized by discrete planar slip-surfaces or narrow (<50 cm) zones of cataclasis (Figure GS-11-7a) that sharply truncate the external  $S_3$  shape fabric. Unlike the NE shears, the NW shears do not contain continuous zones of mylonite and most appear to have been arrested in the early stages of development. Incipient NW shears are typically marked by en échelon arrays of subvertical extension fractures that trend north-northwest (in the western domain) and are quartz filled. In some locations, it is apparent that these extension veins nucleated on, and locally linked, small-scale heterogeneities in the rock mass (Figure GS-11-7b). At a later stage of development, these veins were linked by discrete, through-going slip-surfaces (Figure GS-11-7c). Where present, fault-fill veins tend to be thin and discontinuous, with massive to weakly laminated internal structures (Figure GS-11-7d, e) and local stylolitic pressure-solution seams composed of fine-grained pyrite, tourmaline and/or chlorite.

The lateral tips of the NW shears appear to be mostly defined by NE shears; the resulting lines of intersection typically plunge at steep angles to the north (Figure GS-11-5a, b). Offsets of markers are right lateral and apparent displacements are generally less than 2 m. Diffuse peripheral arrays of en échelon extension fractures vary from planar to prominently sigmoidal (Z-asymmetric; Figure GS-11-7c, d) and are quartz filled. In the western domain, the lateral tips of these fractures typically strike to the north-northwest and dip subvertically (Figure GS-11-3e). Coupled with offsets and dilational jogs, the geometry of the extension veins indicates dextral-normal oblique-slip shear along the NW shears. Slickenlines and chlorite lineations on slip-surfaces plunge steeply or moderately to the northeast, roughly parallel to the  $L_3$  lineation in the NE shears and wallrocks. In contrast, the bulk-slip vector calculated for NW shears in the western domain plunges moderately to the southeast (Figure GS-11-5c), at a significant angle to lineations in the shear planes (Figure GS-11-3d). As with the NE shears, this discrepancy may be due to reactivation or may indicate a non-ideal stress configuration during shearing.

### ***G<sub>4</sub> structures***

Bedding, synvolcanic dikes and  $G_3$  fabrics throughout the mine trend are overprinted by a finely spaced

crenulation cleavage of the  $G_4$  generation. In the western domain, the  $S_4$  cleavage generally strikes to the west-southwest and dips steeply or moderately to the northwest, whereas it strikes southwest and dips steeply northwest in the eastern domain (Figures GS-11-3f, l). In both domains, the  $S_4$  cleavage cuts counter-clockwise across all earlier structures and is particularly apparent in the  $G_3$  high-strain zones (Figure GS-11-4d). The change in orientation of the cleavage mimics that observed for bedding, dikes and the  $S_3$  fabric, indicating that it predates the macroscopic  $F_6$  syncline. The  $S_4$  cleavage produced a prominent crenulation lineation in the plane of the  $S_3$  fabric that parallels the  $L_3$  stretching lineation (for this reason, only the  $L_3$  fabric was routinely recorded in the field). This lineation is also observed on planar structures in the NW and NE shears. The  $S_4$  cleavage is axial planar to rare, open to tight, Z-asymmetric folds of the  $S_3$  fabric. The  $F_4$  hinges plunge moderately to the northeast, subparallel to the  $L_3$  lineation.

### **Discussion and economic significance**

Small-scale examples of NW and NE shears in outcrop show evidence of contemporaneous development under brittle-ductile rheological conditions (Figure GS-11-8a-d). This evidence includes their close spatial association, mutual crosscutting relationships and similarities in the mineralogy and style of associated extension veins. In the western domain, the geometry and kinematics of the shears indicate that they accommodated north-northeast-directed shortening. Here, the NE and NW shears are arranged in a broadly symmetric manner to the  $S_3$ - $L_3$  shape fabric (Figure GS-11-5a). Overprinting relationships indicate that this shortening likely occurred during the late increments of the deformation recorded by the  $S_3$ - $L_3$  shape fabric, which likewise accommodated north-northeast shortening, and prior to the onset of the deformation recorded by the  $S_4$  crenulation cleavage. On a macroscopic scale, this deformation appears to have been strongly partitioned into narrow domains of penetrative non-coaxial shear, which separate wider domains of mostly coaxial shear. The brittle-ductile nature of the late- $G_3$  structures may relate to transiently higher strain rates or fluid pressures, or strain-hardening effects, during the late increments of regional north-northeast shortening.

Within this kinematic framework, the NE shears are interpreted to represent discrete zones of strongly partitioned  $G_3$  non-coaxial strain. These shears transect stratigraphy at shallow counter-clockwise angles and appear to have been controlled, at least in part, by primary anisotropy (dikes) in relatively competent rock types. Kinematic indicators and associated extension-vein arrays indicate sinistral-reverse oblique-slip shear. In contrast, the NW shears transect stratigraphy at oblique clockwise angles and do not appear to be controlled by pre-existing anisotropy. Kinematic indicators and extension-vein arrays

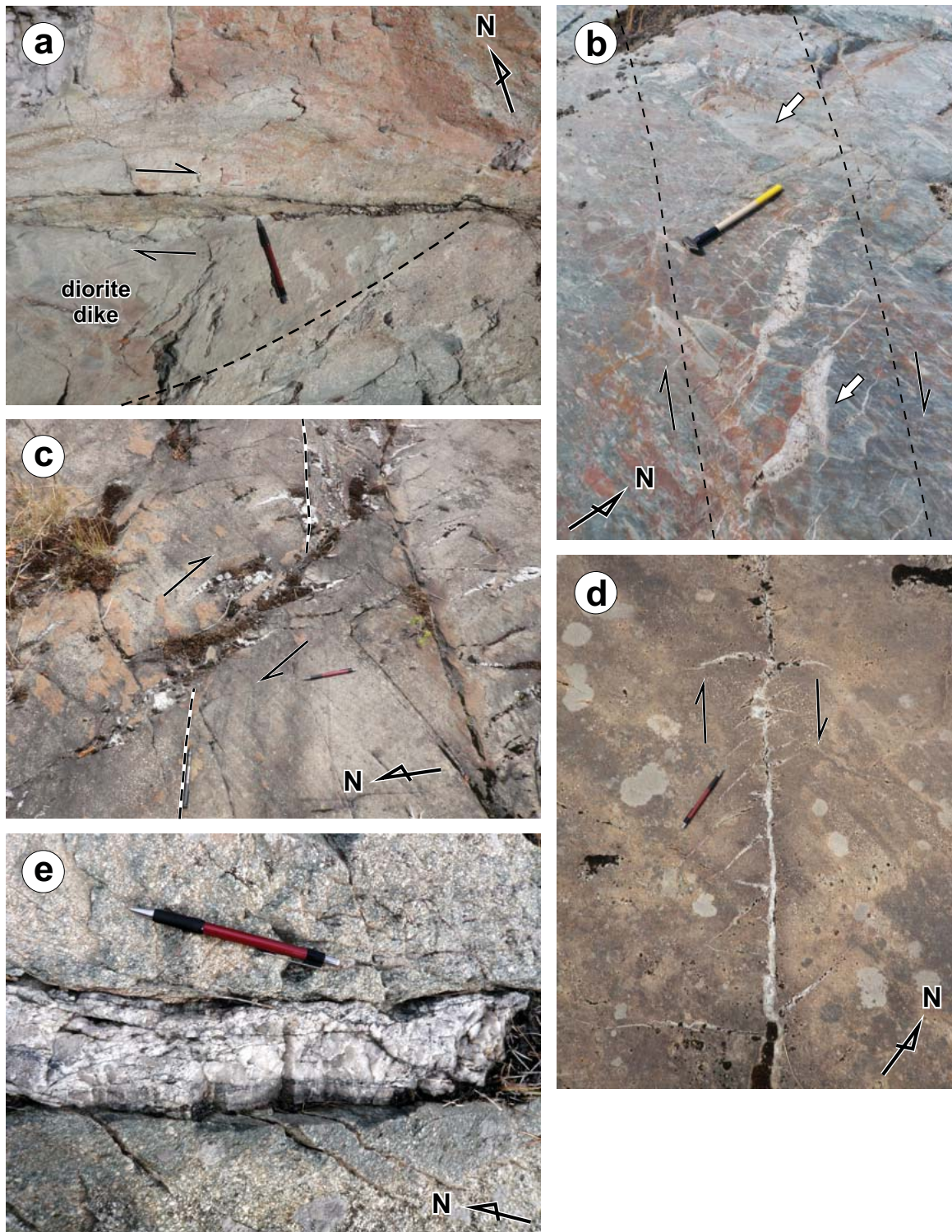


**Figure GS-11-7:** Outcrop photographs of small-scale northwest-trending shears (NW shears): **a)** shear showing discrete slip-surfaces and narrow seam of cataclasite, 400 m east of the Gold Standard/Hinge deposit; intermediate dike in the footwall of the shear is offset ~1.5 m in a right-lateral sense beyond the limit of the photograph; **b)** insipient shear defined by en échelon extension veins that appear to have nucleated on oversized boulders in heterolithic volcanic conglomerate, 700 m north of the San Antonio/Rice Lake deposit; the two boulders indicated by arrows are 'linked' by the long extension vein in the centre of the photo; **c)** shear showing sigmoidal extension veins and discrete slip-surface, 350 m northwest of the Gold Standard/Hinge deposit; vein asymmetry and offset of the volcanic sandstone layer (upper contact indicated by dashed lines) indicate right-lateral movement; **d)** discrete shear showing thin fault-fill vein and peripheral extension veins, 100 m west of the Gold Standard/Hinge deposit; **e)** laminated fault-fill vein in a discrete shear, 350 m north of the San Antonio/Rice Lake deposit.

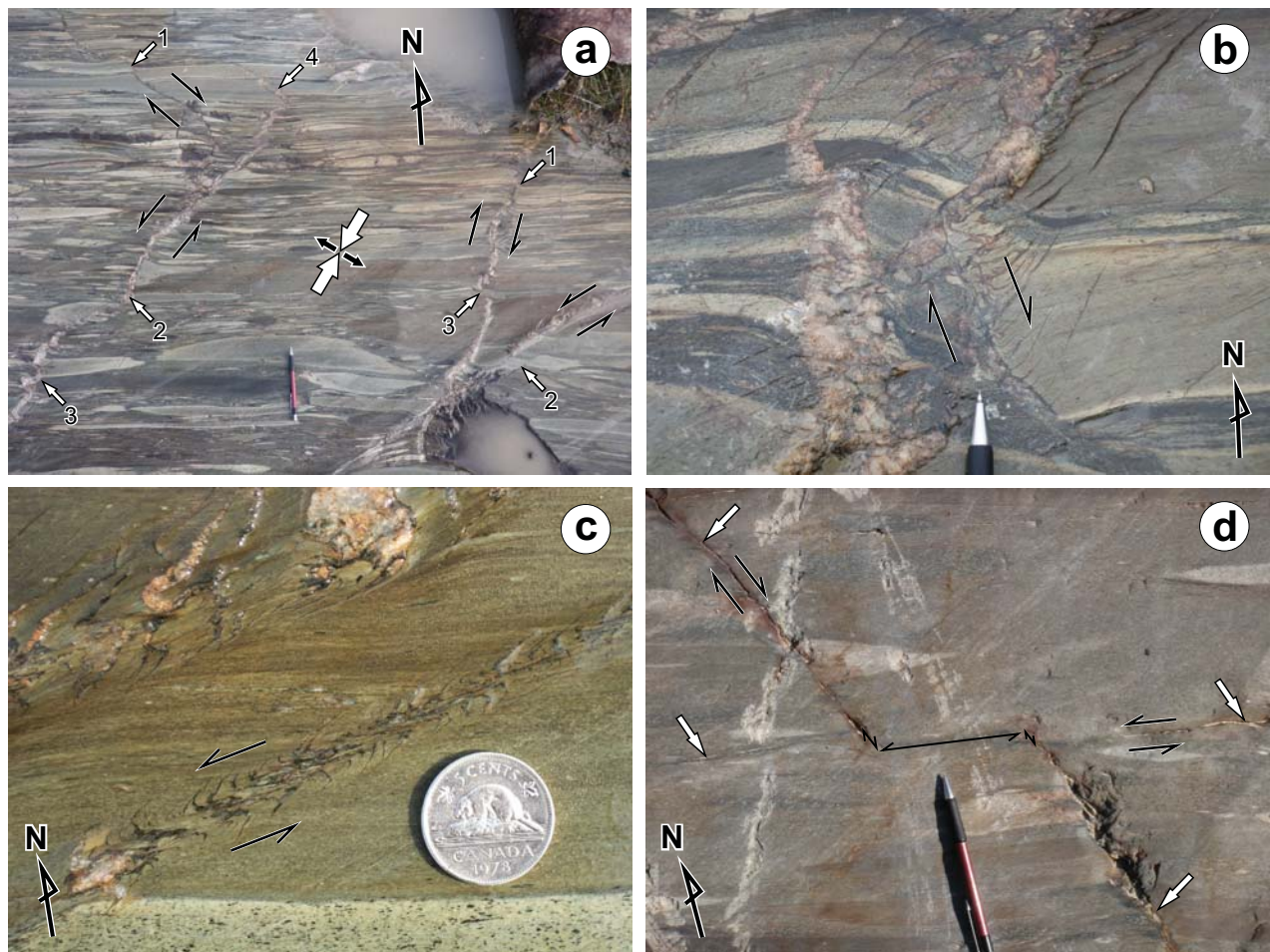


**Figure GS-11-8:** Outcrop photographs showing small-scale examples of northwest-trending shears (NW shears) and northeast-trending shears (NE shears) in volcanic conglomerate along the south margin of the new tailings impoundment, north of Bissett; flattened clasts define the  $S_3$  shape fabric in each photograph: **a)** discrete NW and NE shears, showing dextral offset of markers along NW shears (1), sinistral offset of markers along NE shears (2), ptgmatic folding of fault-fill veins in north-northeast-trending segments of NW and NE shears (3), and wing-crack at lateral tip of NE shear (4); note also the progressive increase in apparent displacement along strike to the southwest in this shear; **b)** detail of NW shear, showing discrete, folded or refracted, slip-surface and peripheral extension fractures; **c)** detail of NE shear, showing sigmoidal extension fractures; **d)** mutual overprinting relationship of discrete NW and NE shears (white arrows); note left-lateral offset of NW shear and right-lateral offsets of NE shear.

associated with the NW shears indicate dextral-normal oblique-slip shear. Mutual crosscutting relationships indicate that the NE and NW shears were coeval and at least locally formed as a conjugate set, as has been proposed for similar structures in the San Antonio/Rice Lake deposit (e.g., Stockwell, 1938; Rhys, 2001). In other locations, the NW shears appear to represent subsidiary structures that accommodated dextral (antithetic) slip during counter-clockwise rotation of rectilinear blocks in domains bounded by NE shears (Figure GS-11-9).

The latter structural geometry is observed at contractional steps in natural fault systems at scales varying from centimetres (e.g., Kim et al., 2004) to tens of kilometres (e.g., Nicholson et al., 1986) and has been reproduced in analogue model experiments of strike-slip faulting in zones of distributed shear deformation (e.g.,

Schreurs, 1994). As shown schematically in Figure GS-11-10, subsidiary structures may record either antithetic or synthetic slip depending on local boundary conditions or factors such as differential slip on the bounding structures. Both models (i.e., conjugate faulting or block rotation) appear to be compatible with the meso- to macroscopic geometry of structures and LiDAR lineaments observed in the mine trend. However, both must be reconciled with the steep orientations of lineations observed in the NW and NE shears, which plunge subparallel to the line of intersection rather than suborthogonally, as would be predicted. Hence, it appears probable that the shears were at least locally reactivated, perhaps with the NW shears serving as compressional oversteps between adjacent NE shears and thus accommodating reverse (northeast-side-up) slip during a later increment of the

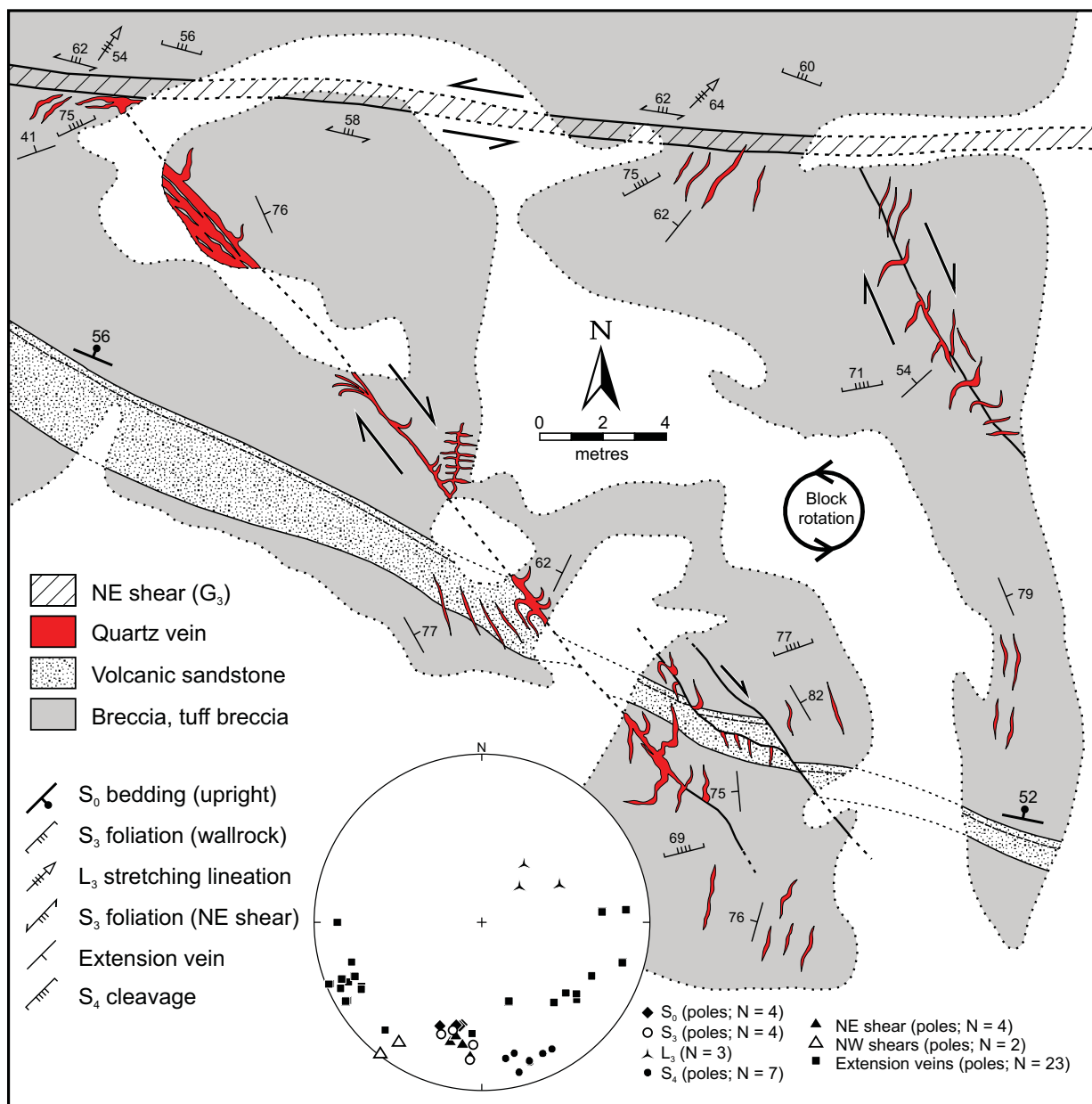


**Figure GS-11-9:** Outcrop map of northwest-trending shears (NW shears) in the footwall of a major northeast-trending shear (NE shear) in the Townsite dacite, approximately 400 m northwest of the Gold Standard/Hinge deposit (UTM Zone 15, 312997E, 5655941N, NAD83). Block rotation is indicated by the slight (10–15°) counter-clockwise deflection of bedding orientations in the shear-bounded block in the eastern portion of the outcrop. Overprinting relationships between the  $S_3$  foliation and  $S_4$  cleavage are particularly well-preserved in the NE shear (e.g., Figure GS-11-4d). An example of a NW shear from this outcrop is provided in Figure GS-11-7c.

$G_3$  deformation (Figure GS-11-10). In the analogue-model experiments of Schreurs (1994), antithetic cross-faults acquired a dip-slip component of displacement in late increments of the progressive shear deformation, and this displacement became more pronounced with increasing bulk shear.

The NE shears exposed in outcrop are comparable in most respects to east-northeast-trending brittle-ductile shears in the San Antonio/Rice Lake mine, which crosscut the thickest portion of a weakly differentiated gabbro sill

that intrudes the lower portion of the Townsite unit and dips moderately to the northeast. The shears dip steeply to the north-northwest and form a right-stepping, en échelon array along the strike of the sill. Sill contacts and intermediate dikes are offset in a left-lateral sense and are locally back-rotated between adjacent shears. Auriferous fault-fill ('16-type') veins within the shears form major tabular orebodies that can be traced along strike for up to 200 m and range up to 2 m thick. Abrupt textural variations (laminated, massive or brecciated) and multiple

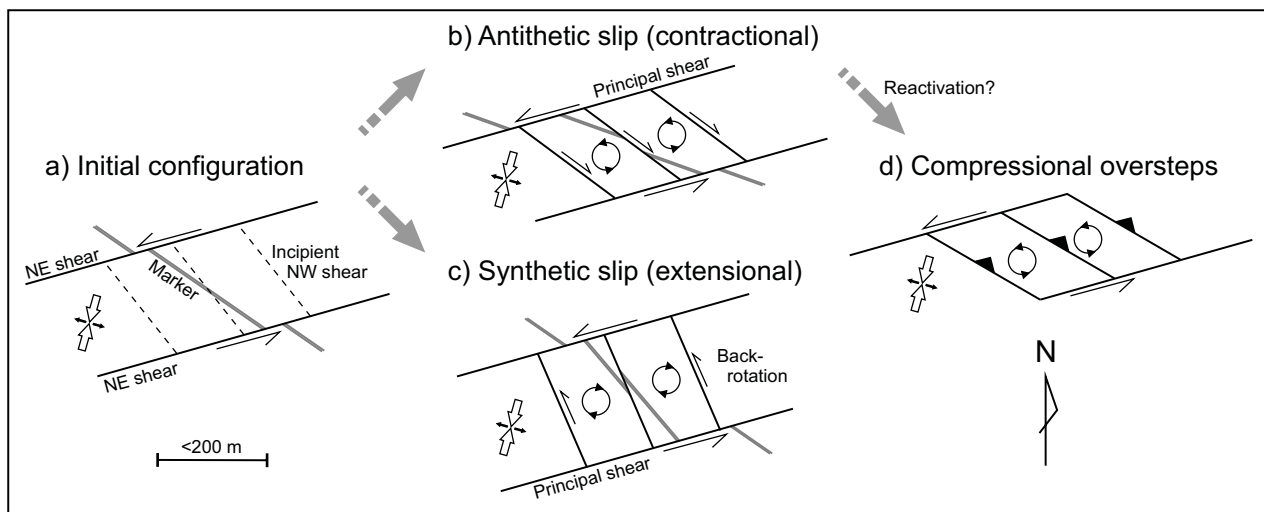


**Figure GS-11-10:** Schematic plan view illustrating the structural geometry of northeast-trending shears (NE shears) and northwest-trending shears (NW shears), and two kinematic models that incorporate differential sinistral slip on adjacent NE shears, crossfaulting and large-scale block rotation in a near-field stress regime of north-northeast-directed compression: **a)** initial configuration; **b)** counter-clockwise rotation of blocks and antithetic slip on NW shears, with resulting contraction across the block-faulted domain; compare to outcrop example in Figure GS-11-9; **c)** clockwise rotation of blocks and synthetic slip on NW shears, with resulting extension across the block-faulted domain; **d)** reactivation (northeast-side-up) of antithetic NW shears in a compressional overstep that joins two NE shears.

generations of planar slip-surfaces, extension fractures and stylolitic pressure-solution seams in these veins indicate repeated cycles of fault-slip, dilation, hydraulic fracturing, hydrothermal sealing and stress accumulation associated with fault-valve behaviour (Sibson et al., 1988; Cox, 1995). The 16-type veins are particularly thick and continuous in large-scale dilational jogs that formed where the host shears refracted into the sill across the hangingwall contact. By analogy, locations where NE shears crosscut the hangingwall contacts of relatively competent rock units, or units with a pronounced internal strength-anisotropy (e.g., bedding or discordant dikes), should be considered particularly favourable targets for surface exploration. The surface exposure of the Gold Standard/Hinge deposit is the best example of this style of vein in outcrop.

The NW shears exposed in outcrop are interpreted to be analogous to the structures that host major northwest-trending orebodies (38-type veins) in the San Antonio/Rice Lake mine. The 38-type veins strike roughly parallel, or slightly clockwise, to the northwest-trending gabbro sill. In the upper levels of the mine, subvertical 38-type veins are arranged en échelon down the dip of the sill and are limited in dip extent by the sill contacts. At depth, however, these veins have variable orientations and locally define open sigmoidal folds, perhaps as a result of block rotation and/or distributed shear between the bounding NE shears. Incipient 38-type veins are controlled by discrete brittle faults, along which intermediate dikes are offset in a right-lateral sense. Fully developed 38-type veins range up to 500 m in strike length and up to 10 m in thickness,

and typically exhibit complex internal structures. Sinuous zones of hydrothermal breccia in the core of the veins typically transition outward into complex stockwork zones and peripheral arrays of moderately north-dipping extension veins. Local jigsaw-fit textures of angular wallrock fragments in the breccia veins indicate in situ fragmentation during intense hydraulic fracturing. Fault-fill veins are preserved locally in the central portions of the 38-type veins but tend to lack the well-developed laminar texture of the 16-type veins. Outside of the San Antonio/Rice Lake deposit, the only known occurrence of a well-developed '38-type' vein system is the historical Wingold deposit (No. 1 vein; Stockwell, 1938). Nevertheless, the widespread occurrence of NW shears suggests that '38-type' veins may be far more abundant than is presently indicated. Structural domains showing evidence of block-rotation (e.g., deviation of bedding or dike orientations from regional trends) should be considered particularly favourable exploration targets.

## Acknowledgments

The author thanks A. Piotrowski (University of Manitoba) for enthusiastic and very capable assistance in the field; L. Chackowsky, M. Pacey and B. Lenton (MGS) for cartographic, GIS and drafting support; N. Brandson and E. Anderson (MGS) for efficient expediting services; T. Lewis and P. Theyer (Wildcat Exploration Ltd.) for facilitating access to accommodations in Bissett; D. Ginn and R. Boulay (San Gold Corp.) for providing free access to the mine property and proprietary data; D. Berthelson, S. Horte and A. Kathler (San Gold Corp.) for providing

the author with a geological overview and underground tour of the Hinge, L10 and 007 deposits; and S. Gagné (MGS) for reviewing the manuscript.

## References

- Anderson, S.D. 2004: Preliminary results and economic significance of geological mapping and structural analysis in the Rice Lake area, central Rice Lake greenstone belt, Manitoba (NTS 52M4 and 52L13); *in* Report of Activities 2004, Manitoba Industry, Economic Development and Mines, Manitoba Geological Survey, p. 216–231.
- Anderson, S.D. 2005: Geology and structure of the Rice Lake area, Rice Lake greenstone belt, Manitoba (part of NTS 52M04 and 52L13); Manitoba Industry, Economic Development and Mines, Manitoba Geological Survey, Preliminary Map PMAP2005-1, scale 1:20 000.
- Anderson, S.D. 2008: Geology of the Rice Lake area, Rice Lake greenstone belt, southeastern Manitoba (parts of NTS 52L13, 52M4); Manitoba Science, Technology, Energy and Mines, Manitoba Geological Survey, Geoscientific Report GR2008-1, 97 p.
- Anderson, S.D. 2011: Geology and structure of the Rice Lake mine trend, Rice Lake greenstone belt, southeastern Manitoba (part of NTS 52M4); Manitoba Innovation, Energy and Mines, Manitoba Geological Survey, Preliminary Map PMAP2011-3, scale 1:5000.
- Blenkinsop, T.G. 2008: Relationship between faults, extension fractures and veins, and stress; *Journal of Structural Geology*, v. 30, p. 622–632.
- Cox, S.F. 1995: Faulting processes at high fluid pressures: an example of fault valve behaviour from the Wattle Gully Fault, Victoria, Australia; *Journal of Geophysical Research*, v. 100, p. 12 841–12 859.
- George, P.T. 2010: Mineral reserves, mineral resources and economic assessment, Rice Lake project, Rice Lake greenstone belt, Bissett, Manitoba, for San Gold Corporation; unpublished technical report prepared by GeoEx Ltd., 192 p., URL <<http://www.sangold.ca/i/pdf/2010-oct-43-101.pdf>> [October 2011].
- Gibson, J.C. and Stockwell, C.H. 1948: San Antonio mine; *in* Structural Geology of Canadian Ore Deposits, Canadian Institute of Mining and Metallurgy, Geology Division, Symposium Volume, p. 315–321.
- Kim, Y-S., Peacock, D.C.P. and Sanderson, D.J. 2004: Fault damage zones; *Journal of Structural Geology*, v. 26, p. 503–517.
- Lau, M.H.S. 1988: Structural geology of the vein system in the San Antonio gold mine, Bissett, Manitoba, Canada; M.Sc. thesis, University of Manitoba, Winnipeg, Manitoba, 154 p.
- Lau, M.H.S. and Brisbin, W.C. 1996: Structural geology of the San Antonio mine, Bissett, Manitoba; Geological Survey of Canada, Open File 1699, 65 p.
- Nicholson, C., Seeber, L., Williams, P. and Sykes, L.R. 1986: Seismic evidence for conjugate slip and block rotation within the San Andreas fault system, southern California; *Tectonics*, v. 5, p. 629–648.
- Percival, J.A., McNicoll, V. and Bailes, A.H. 2006a: Strike-slip juxtaposition of ca. 2.72 Ga juvenile arc and >2.98 Ga continent margin sequences and its implications for Archean terrane accretion, western Superior Province, Canada; *Canadian Journal of Earth Sciences*, v. 43, p. 895–927.
- Percival, J.A., Sanborn-Barrie, M., Skulski, T., Stott, G.M., Helmstaedt, H. and White, D.J. 2006b: Tectonic evolution of the western Superior Province from NATMAP and LITHOPROBE studies; *Canadian Journal of Earth Sciences*, v. 43, p. 1085–1117.
- Poulsen, K.H., Ames, D.E., Lau, S. and Brisbin, W.C. 1986: Preliminary report on the structural setting of gold in the Rice Lake area, Uchi Subprovince, southeastern Manitoba; *in* Current Research, Part B, Geological Survey of Canada, Paper 86-1B, p. 213–221.
- Reid, J.A. 1931: The geology of the San Antonio gold mine, Rice Lake, Manitoba; *Economic Geology*, v. 26, p. 644–661.
- Rhys, D.A. 2001: Report on a structural geology study of the, San Antonio Mine, Bissett, Manitoba; prepared for Harmony Gold (Canada) Inc.; unpublished technical report prepared by Panterra Geoservices Inc., 74 p., URL <<http://www.sangold.ca/i/pdf/2001Mar-PSGReport.pdf>> [October 2011].
- Schreurs, G. 1994: Experiments on strike-slip faulting and block rotation; *Geology*, v. 22, p. 567–570.
- Sibson, R.H., Robert, F. and Poulsen, K.H. 1988: High-angle reverse faults, fluid-pressure cycling, and mesothermal gold-quartz deposits; *Geology*, v. 16, p. 551–555.
- Stockwell, C.H. 1938: Rice Lake–Gold Lake area, southern Manitoba; Geological Survey of Canada, Memoir 210, 79 p.